Received: 25 September 2020 | Revised: 21 February 2021 | Accepted: 22 February 2021

DOI: 10.1111/joa.13426

Journal of Anatomy ANATOMICAL SOCIETY WILEY

ORIGINAL PAPER

Digital dissection of the head of the frogs *Calyptocephalella gayi* and *Leptodactylus pentadactylus* with emphasis on the feeding apparatus

Stephanie Kunisch[1] | **Valentin Blüml**[1] | **Thomas Schwaha**[1] | **Christian Josef Beisser**[1] | **Stephan Handschuh**[2] | **Patrick Lemell**[1]

[1]Department of Evolutionary Biology, Faculty of Life Sciences, University of Vienna, Vienna, Austria

[2]VetCore, University of Veterinary Medicine Vienna, Vienna, Austria

Correspondence
Patrick Lemell, Department of Evolutionary Biology, Faculty of Life Sciences, University of Vienna, Vienna, Austria.
Email: patrick.lemell@univie.ac.at

Abstract

Micro-computed tomography (microCT) of small animals has led to a more detailed and more accurate three-dimensional (3D) view on different anatomical structures in the last years. Here, we present the cranial anatomy of two frog species providing descriptions of bone structures and soft tissues of the feeding apparatus with comments to possible relations to habitat and feeding ecology. *Calyptocephalella gayi*, known for its aquatic lifestyle, is not restricted to aquatic feeding but also feeds terrestrially using lingual prehension. This called for a detailed investigation of the morphology of its feeding apparatus and a comparison to a fully terrestrial species that is known to feed by lingual prehension such as *Leptodactylus pentadactylus*. These two frog species are of similar size, feed on similar diet but within different main habitats. MicroCT scans of both species were conducted in order to reconstruct the complete anatomical condition of the whole feeding apparatus for the first time. Differences in this regard are evident in the tongue musculature, which in *L. pentadactylus* is more massively built and with a broader interdigitating area of the two main muscles, the protractor musculus genioglossus and the retractor musculus hyoglossus. In contrast, the hyoid retractor (m. sternohyoideus) is more massive in the aquatic species *C. gayi*. Moreover, due to the different skull morphology, the origins of two of the five musculi adductores vary between the species. This study brings new insights into the relation of the anatomy of the feeding apparatus to the preferred feeding method via 3D imaging techniques. Contrary to the terrestrially feeding *L. pentadactylus*, the skeletal and muscular adaptations of the aquatic species *C. gayi* provide a clear picture of necessities prescribed by the habitat. Nevertheless, by keeping a certain amount of flexibility of the design of its feeding apparatus, *C. gayi* is able to employ various methods of feeding.

KEYWORDS
amphibian, anura, cranial anatomy, hyoid apparatus, micro-computed tomography, skull, tongue

Stephanie Kunisch and Valentin Blüml contributed equally to the manuscript.

1 | BACKGROUND

Since the beginning of this century, morphological studies hugely profited from advances in imaging techniques such as X-ray computed tomography (CT) and from image processing and analysis tools. Initially, X-ray CT was used to study high-density materials such as the mineralized vertebrate skeleton (Bever et al., 2005; Carpenter et al., 2004; Maisano et al., 2002; Rowe et al., 2005) or fossils (Polcyn et al., 2002; Tykoski et al., 2002), which can be easily visualized via thresholding or other automatic segmentation methods. This enabled fast and easy visualization of skeletons of geometrically undistorted datasets, compared with traditional physical sectioning techniques or drawings based on destructive dissections.

In contrast, non-mineralized tissue shows poor X-ray contrast and only became feasible for CT imaging by the advent of new staining techniques (Gignac et al., 2016; Metscher, 2009). Soft tissue staining allows accurate three-dimensional (3D) reconstructions of muscles, cartilages and other non-mineralized tissues. Intensities of stained soft tissues, however, often overlap with skeletal structures, which impedes easy visualization of mineralized structures alone. This problem was partially overcome by microscopic dual-energy CT (microDECT) imaging protocols that allow automatic spectral separation of mineralized tissue and stained soft tissues (Handschuh et al., 2017) and enable effective segmentation and fast visualization of, for example, musculoskeletal systems (Schwarz et al., 2020).

To date, micro-computed tomography (microCT) is a suitable tool for a wide range of specimen sizes (Handschuh et al. 2019; Holliday et al., 2013; Sullivan et al., 2019) and becomes more widespread in vertebrate morphology. Such datasets are referred to as digital dissections (Brocklehurst et al., 2019; Collings & Richards, 2019; Cox & Faulkes, 2014; Jones et al., 2019; Klinkhamer et al., 2017; Lautenschlager et al., 2014; Porro & Richards, 2017) that provide several advantages: (i) inclusion of annotations for bones, muscles and a variety of other organs for comparative or teaching purposes, (ii) availability as interactive *.PDF files for enhanced understanding of 3D structures and comparison to other species and (iii) deposition of the original image data (i.e. CT scans) in online repositories such as DigiMorph (www.digimorph.org) or MorphoSource (www.morphosource.org), which are open access and for anyone to use for teaching or research purposes.

Extant amphibians (http://amphibiaweb.org) comprise ~6.700 anurans, which is about 90% of the whole class, and around one-fifth of all extant tetrapods (Jetz & Pyron, 2018). Digital dissections are rare among frogs. Some exemplary studies include cranial anatomy of tadpoles (Haas et al. 2014), tongue musculature and surface structure (Kleinteich & Gorb, 2015a, 2015b), comparison of appendicular skeleton in recent and fossil frogs (Matthews & du Plessis, 2016) and myoanatomical reconstructions of *Xenopus laevis* (Porro & Richards, 2017). Recent studies focused on the osteology of a fossorial frog (Zhang et al. 2019), humerus of burrowing frogs (Keeffe & Blackburn, 2020) and the description of the pelvic and hind limb skeleton in relation to frog locomotion (Buttimer et al, 2020). These fragmentary datasets call for a more holistic digital dissection that includes mineralized (bone) and unmineralized (cartilage) skeletal elements, musculature and associated structures. For creating such a dissection dataset, the cranial anatomy with focus on the feeding apparatus of two frogs that live in different habitats—water versus land—but feed on the same diet are reconstructed and compared.

The helmeted water toad, *Calyptocephalella gayi* (Strand, 1928), is part of the small family Calyptocephalellidae and the only extant species (Jetz & Pyron, 2018; Pyron & Wiens, 2011). It is a large aquatic frog that lives in rivers, lakes and ponds in the lowlands of Chile (Cei, 1962; Hutchins et al., 2003) and feeds on aquatic insect larvae, fish, other frogs, small birds and mammals (Hutchins et al., 2003; Wampula, 2015). Until recently, *C.gayi* was thought to feed aquatically using jaw prehension and forearm scooping (Gray et al., 1997; O'Reilly et al., 2002), but Wiesinger (2017) described them using suction feeding with a simultaneous movement of their forearms for sealing off the mouth opening to avoid escape of the prey. Interestingly, even though it is a purely aquatic species, *C.gayi* is also able to feed on land as a mechanical puller (Nishikawa, 2000). However, Wiesinger (2017) observed jaw prehension, frequently in combination with tongue protraction, more often than pure lingual prehension.

Leptodactylus pentadactylus (Laurenti, 1768), the South American bullfrog, belongs to the large family of Leptodactylidae (De Sá et al., 2014; Pyron & Wiens, 2011). This terrestrial species lives not only in the tropical rainforests but also in dry lower montane forests of northern South America (Hutchins et al., 2003) and also feeds on large prey like arthropods, frogs, lizards, small birds and mammals. Nishikawa (2000) also described *L.pentadactylus* as a mechanical puller, but there is no information whether aquatic feeding occurs.

This study compares the feeding anatomy of the aquatic *C.gayi* and the terrestrial *L.pentadactylus*. The state-of-the-art image visualization techniques provide a detailed view on skeleton and soft tissues. By analysing their similarities and differences, insights into possibly relevant morphological features that enable the use of certain feeding methods were gathered.

2 | MATERIAL AND METHODS

Similar-sized frog specimens were provided by the National History Museum Vienna (*Calyptocephalella*: NMW 40237:4, 6 cm, sex unknown; NMW40237:8, 8 cm, female; *Leptodactylus*: NMW 33748:2, 7 cm, male). MicroCT scans were conducted with an Xradia MicroXCT-400 (Carl Zeiss X-ray Microscopy, Pleasanton, CA, USA) using the 0.4× macro-detector assembly. All specimens were young adults and probably not entirely ossified, indicating that older specimens might have more ossified skulls and hyoids than those in the current analysis. For soft tissue discrimination, we chose to stain the specimens using iodine compounds. For the given sample sizes of several centimetres, iodine staining provides superior contrast for simultaneously visualizing different kinds of non-mineralized tissues (muscles, cartilages and others) compared with other approaches for contrast enhancement such as propagation-based phase-contrast tomography.

Two specimens of *C.gayi* were scanned. The first specimen (NMW40237:8) was mounted in 40% ethanol (EtOH) to visualize the ossified structures. For soft tissue visualization, a second specimen of *C.gayi* (NMW40237:4) was washed in distilled water, stained in 0.25% iodine (I_2) and 0.5% potassium iodide (KI) solution in distilled water for 4 weeks and finally washed and mounted again in distilled water. One specimen of *L.pentadactylus* (NMW33748:2) was dehydrated to 100% EtOH and stained for 4 weeks in 1% I_2 in 100% EtOH. It was washed and mounted in 100% EtOH. At this point, it should be noted that we initially planned to stain both species with aqueous Lugol's I_2KI solution. However, after observing notable decalcification in the *C.gayi* specimen stained with aqueous I_2KI, we decided to stain the *L.pentadactylus* specimen with elemental iodine in ethanol in order to preserve the bone mineral. Decalcification occurring in museum specimens after long-term storage in 70% ethanol and staining in aqueous I_2KI solution was recently described in detail by Early et al. (2020).

All specimens were mounted for scanning in a vertical position in plastic containers filled with the respective liquid (distilled water, 40% EtOH or 100% EtOH, as described above). Inside the plastic containers, specimens were stabilized with lab tissue paper. All specimen manipulations were made with the greatest care in order to prevent any mechanical distortions of the specimens.

The unstained *C.gayi* specimen was scanned at 70 kVp/114 µA with an exposure time of 20 s per projection and isotropic voxel size of 29.61 µm. The I_2KI-stained *C.gayi* specimen was scanned at 60 kVp/133 µA with an exposure time of 30 s and a voxel size of 17.16 µm. The *L.pentadactylus* specimen was imaged using microDECT, which utilizes two different energy spectra to improve the differentiation between soft and mineralized tissues (Supplement 1; for a detailed explanation, see Handschuh et al., 2017). X-ray source settings for the microDECT scan of *L.pentadactylus* were 40 kVp and 200 µA (low energy, 60-s exposure per projection) and 80 kVp and 100 µA (high energy, 30-s exposure). Voxel size was 21.15 µm. All scans were recorded with an angular increment of 0.17°.

CT stacks were analysed and reconstructed with Amira 6.4 (FEI, Oregon, USA). The general outline of the head and ossified structures was visualized as volume rendering, whereas specific structures of the feeding apparatus (hyoid, tongue, muscles) were segmented and visualized as surface rendering. Figure plates were compiled with Photoshop (Adobe Photoshop Elements 11, Adobe Systems, Delaware, USA).

3 | RESULTS

3.1 | Morphology of skeletal elements and the tongue

The bony part of the skull of *C.gayi* is more massively built, showing no reductions on the roof compared with *L.pentadactylus*. The greatest width of the skull is 1.3 times its total length and approximately three times its height—for the analysed specimen it is 2.3 cm wide, 1.8 cm long and 0.8 cm high. In *L.pentadactylus*, the width is 1.2 times its length and 3.4 times its height—for the analysed specimen: 3.1 cm wide, 2.6 cm long and 0.9 cm high (Figure 1). Owing to these size differences, *C.gayi* has a comparatively shorter and flatter skull. The lateral side, built by the maxillar and squamosal, is firmly attached to the nasal and frontoparietal bone, whereas these bridges are completely reduced in *L.pentadactylus* (Figure 1a,d; Supplement 2a,e). Only the squamosal of *Leptodactylus* is fully ossified and embedded into the cartilaginous skull. The external surface of the skull of *C.gayi* is coarsely sculptured with tubercles, ridges and pits together with some vascular openings (Figure 1a,b, Supplement 3), while that of *L.pentadactylus* is comparatively smooth. The teeth of *C.gayi* are longer (1 mm for the presented specimen vs 0.7 mm) and about half the number compared with *L.pentadactylus*. Furthermore, *C.gayi* has fewer teeth on the vomers that are also less pronounced and located more anterior than in *L.pentadactylus* (Figure 1c,f). Overall, the buccal cavity and the palate are more streamlined in *C.gayi* (Supplement 4).

The hyoid apparatus (Figure 2; Supplement 5) of *C.gayi* is markedly broader than that of *L.pentadactylus*. All processes of the former show the same enlarged pattern. The anterior hyale processes enclose the hyoglossal musculature that runs through the narrow hyoglossal sinus (Figure 2c,g). In *L.pentadactylus*, this musculature is larger, and thus, the space between the anterior hyale processes is not restricted as in *C.gayi*. Laterally ensuing, the ceratohyals of both form a wide curve (more pronounced in *C.gayi*) running caudally to their attachment site on the posterior area of the otical region (Supplement 2d,h). The anterolateral (or alary) process of *C.gayi* is hammer shaped and fits into the space between the hyale process and the hyoid plate (Figure 2b,c). In contrast, the alary process of *L.pentadactylus* is much smaller and club shaped (Figure 2f,g). The posterolateral and posteromedial processes are also more massively developed than those of *L.pentadactylus*. Consequently, the distance between the anterolateral and the posterolateral processes is greater in the latter, leaving a larger insertion area for the anterior petrohyoid muscle (Figure 2b,f, Figure 4b,f; Supplement 5). In both frogs, the posteromedial processes are ossified—an osseous cuff encloses the cartilage of the process from the dorsal side—and provide the origin for laryngeal musculature. In *L.pentadactylus*, a small adjacent ossified area on the hyoid plate can also be found (Figure 1f).

The tongue of *C.gayi* fills the anterior part of the buccal cavity and lies flat against the vomer and the palate (Supplement 4). It appears bulky and fits exactly into the roof of the mouth. In *L.pentadactylus*, the tongue lies flat on the bottom of the mouth and stretches further posterior. In both frogs, half of the tongue lies in front of the hyoid apparatus, with the other half lying on top of it. The length to width ratio for *C.gayi* is 0.9 and 1.3 for *L.pentadactylus*, which seems to be correlated with the elongated snout.

3.2 | Musculature of the feeding apparatus

This study uses the terminology of the adductor mandibulae muscles proposed by Johnston (2011). The musculus depressor mandibulae (MDM) has an extensive origin from the fascia of the epaxial musculature to the posterior end of the otic capsule and in both

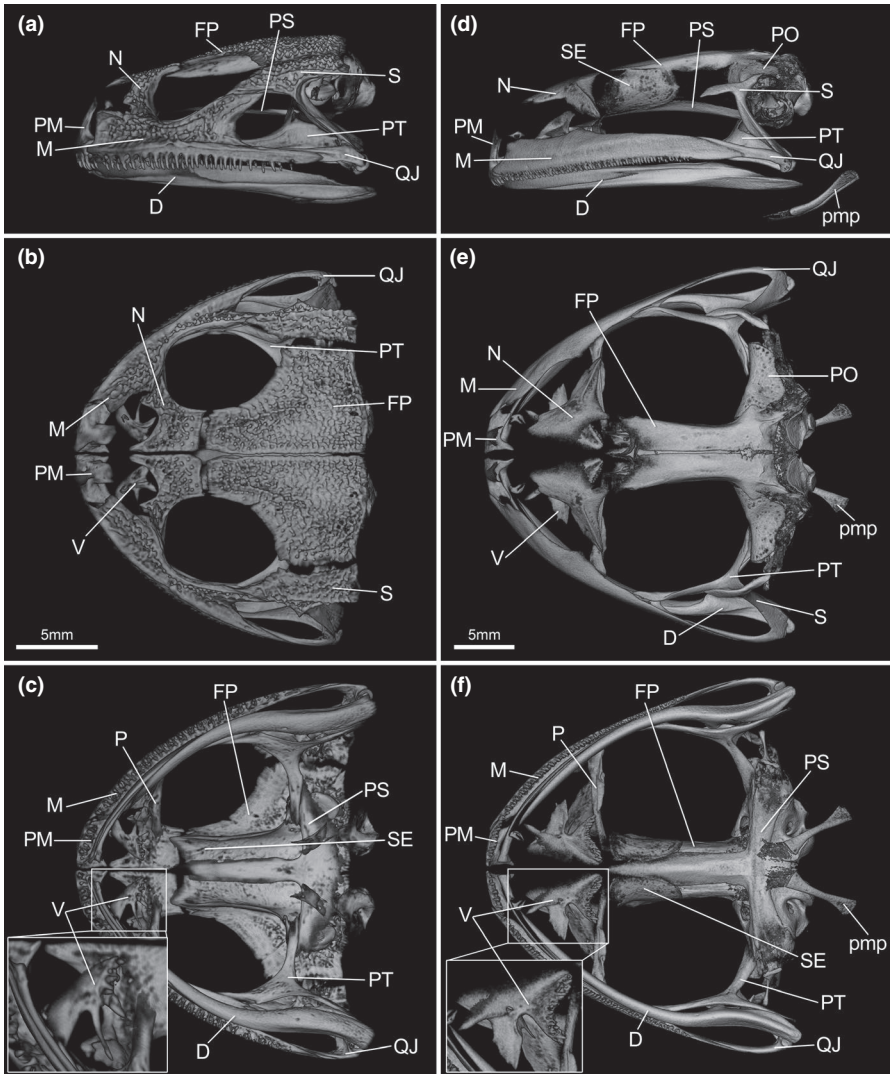

FIGURE 1 Volume rendering of CT data of the skull of *Calyptocephalella gayi* (a-c) and *Leptodactylus pentadactylus* (d-f). (a and d) Lateral view; (b and e) dorsal view; (c and f) ventral view with zoom into vomer region. D, dentale; FP, frontoparietale; M, maxillare; N, nasale; P, palatinum; PM, praemaxillare; pmp, posteromedial process of the hyoid; PO, prooticum; PS, parasphenoid; PT, pterygoid; QJ, quadratojugale; S, squamosum; SE, sphenethomid; V, vomer. Scale bar in b is for *C. gayi*, Scale bar in e is for *L. pentadactylus*

species inserts at the terminal end of the mandible the retroarticular process behind the jaw articulation (Figure 3). It is triangular in shape but caudally more fanned out in *C. gayi* than in *L. pentadactylus*. The anterior part of this muscle originates from the posterior side of the tympanic annulus in *C. gayi*. In contrast, a process on the posterior area of the prootic close to the annulus serves as origin in *L. pentadactylus* (Figure 3d). Furthermore, some bundles originate from the fascia of the m. adductor mandibulae (MAM) longus. This muscle dorsally crosses the tympanum to the prooticum, leading to posteriorly directed fibres. In *C. gayi*, this muscle directly runs from the ventral side of the frontoparietal to the mandible (Figure 3b, Supplement 6). Furthermore, the MAM lateralis is positioned further rostrally and yields a larger gap towards the MDM (Figure 3a,d).

In both frogs, five MAM portions can be differentiated: from lateral to medial, these are MAM lateralis, externus, posterior, longus and internus (Figure 3). The most significant difference between the adductor muscles of *C. gayi* and *L. pentadactylus* are their origin and their subsequent traverse. The MAM lateralis is similar in both species, except the above-mentioned greater rostral and caudal extension in *L. pentadactylus*. This muscle runs from the lower end of the squamosal to the lateral side of the mandible and serves as lateral fixation of the jaw joint (Figure 3a,d). The MAM externus originates from the squamosal, that is, underneath the vertical bar of the T-shaped bone at the height of the tympanum (Figure 3a,d). In *L. pentadactylus*, it additionally originates from the otical region next to the squamosal. In *C. gayi*, it attaches to the dorsal side of the mandible and inserts anteriorly of the MAM lateralis. In *L. pentadactylus*, it is larger and more oblique owing to the rostral extension of the MAM lateralis. The insertion area is more dorsolaterally located in comparison with *C. gayi*. The MAM posterior originates in between these two muscles from the squamosal and inserts on the dorsal side of the mandible just anterior to the jaw articulation

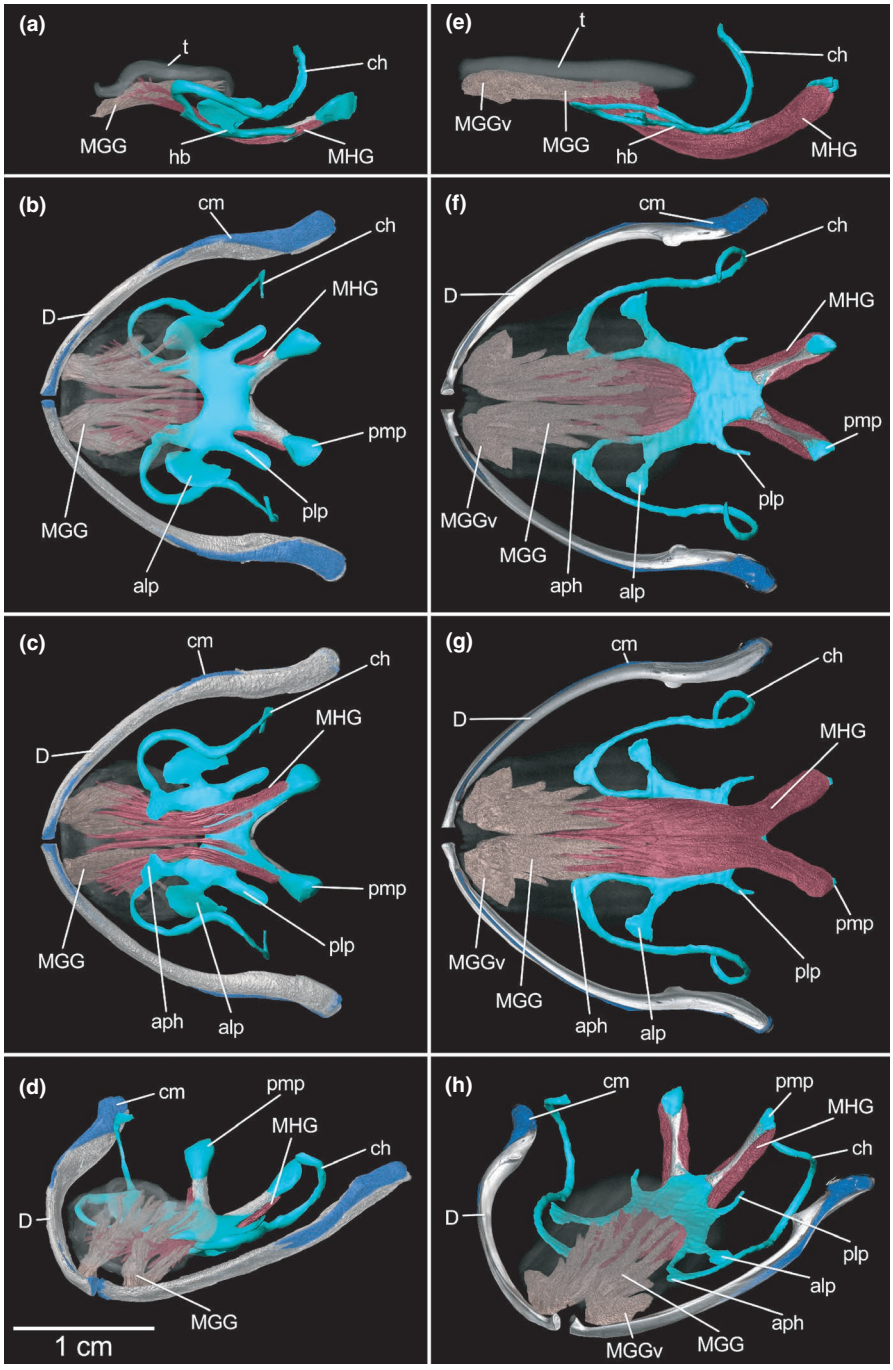

FIGURE 2 Hyoid apparatus including tongue musculature and tongue of *Calyptocephalella gayi* (a-d) and *Leptodactylus pentadactylus* (e-h) based on CT data. Osseous structures are visualized as volume rendering, cartilage and muscles based on segmentation-based rendering (surface or volume). (a and e) Lateral view; (b and f) dorsal view with lower jaw (bone [silver] and cartilage [dark blue]); (c and g) ventral view; (d and h) oblique view from dorsolateral. alp, anterolateral process of the hyoid; aph, anterior process of hyoid; ch, ceratohyale; cm, cartilago meckeli; D, dentale; hb, hyoid body; MGG, musculus genioglossus; MGGv, musculus genioglossus ventralis; MHG, musculus hyoglossus; plp, posterolateral process of the hyoid; pmp, posteromedial process of hyoid; t, tongue. Scale bar applies for a-h

(Figure 3a,d). In *C. gayi*, the insertion area is dorso-median, whereas in *L. pentadactylus* it is dorsal. Proportionally, the MAM longus is the largest adductor followed by the MAM internus and the remaining ones. Both together—longus and internus—comprise about 80% of the MAM muscle mass. In *L. pentadactylus*, these two muscles completely occupy the gap between the orbital region and the MDM, whereas in *C. gayi* they are consecutively stacked behind the orbita, with the MAM internus lying on the most inner side (Figure 3b,e, Supplement 6). In the latter species, the longus muscle originates below the broad frontoparietal, whereas the MAM internus comes from the cartilaginous neurocranium and lies slightly medially to the MAM longus origin (Supplement 6). In *L. pentadactylus*, the MAM

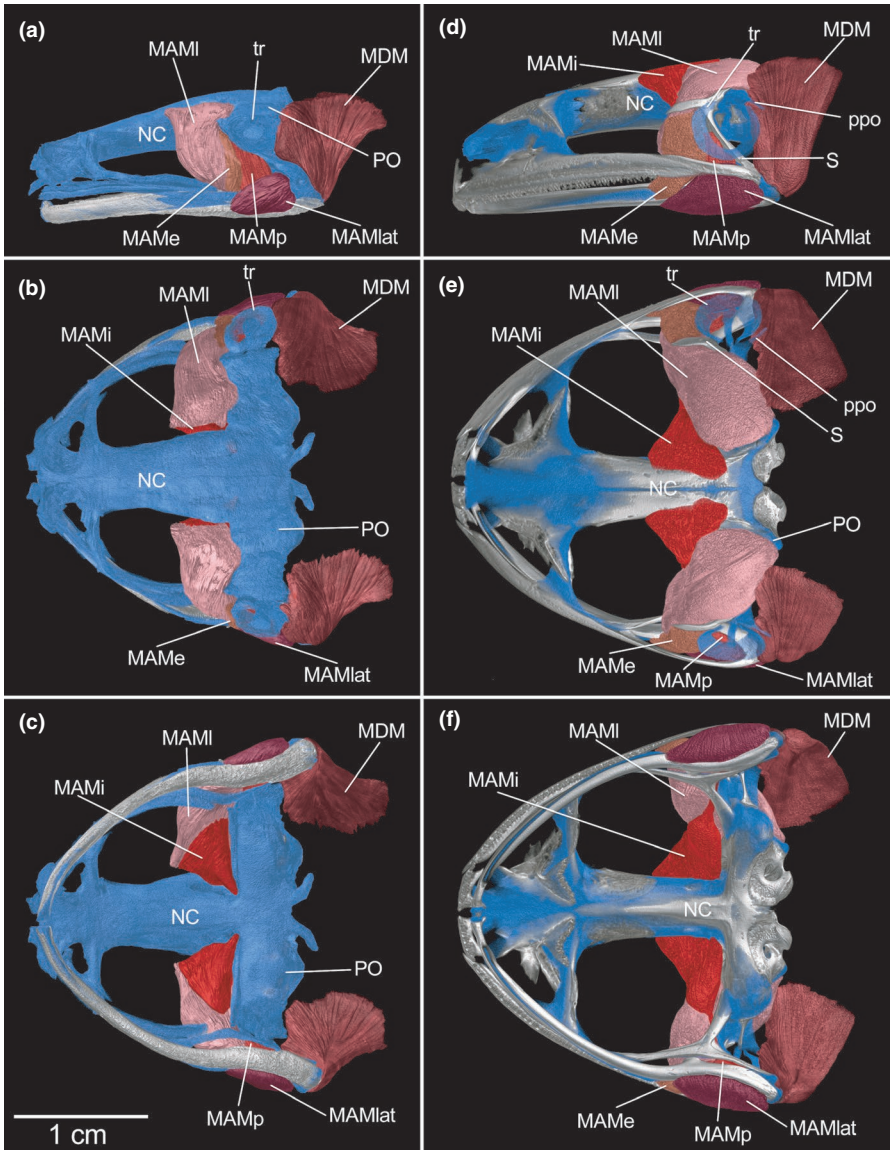

FIGURE 3 Skulls with adductor musculature of *Calyptocephalella gayi* (a-c) and *Leptodactylus pentadactylus* (d-f) based on CT data. Osseous structures are visualized as volume rendering, cartilage and muscles based on segmentation-based rendering (surface or volume). (a and d) Lateral view; (b and e) dorsal view; (c and f) ventral view. MAMe, musculus adductor mandibulae externus; MAMi, musculus adductor mandibulae internus; MAMl, musculus adductor mandibulae longus; MAMlat, musculus adductor mandibulae lateralis; MAMp, musculus adductor mandibulae posterior; MDM, musculus depressor mandibulae; NC, neurocranium; PO, prooticum; ppo, processus prootici; S, squamosum; tr, tympanic ring. Scale bar applies for a-f

longus originates broadly from the dorsal side of the prootic and the caudal part of the frontoparietal. The MAM internus origin is on the frontoparietal, clearly rostrally to the MAM longus (Figure 3e). The parts of both sides of the muscle are connected above the narrow frontoparietal via a fascia (Supplement 6). The insertion of the MAM longus is in both frogs rostrally of the MAM posterior on the mandible, in *L.pentadactylus* the insertion is dorsal, and in *C.gayi* more on the dorso-median side of the lower jaw. The MAM internus of *L.pentadactylus* extends with a slender tendon over the pterygoid to insert on the medial side of the mandible between the MAM longus and posterior. In *C.gayi*, no such tendon can be distinguished; the MAM internus unites with the MAM longus and inserts on the dorso-medial side of the mandible.

Regarding the ventral hyoid musculature (Figure 4), the m. geniohyoideus (MGH) consists of two parts, a medial and a lateral one. In *L.pentadactylus*, the pairs of the MGH medialis were not clearly separable from each other in the CT scan; thus, they have been reconstructed as one (Figure 4f,g). Both originate on the ventral side of the hyoid and insert near the mandible symphysis. The lateral portions of the MGH run from ventral of the posterolateral processes of the hyoid below the anterolateral processes towards the mandibles, whereas the medial parts arise from the posteromedial processes where they partly envelop the ventral portion of the m. hyoglossus (MHG) (Figure 4c,g). In *L.pentadactylus*, this muscle reaches almost the distal end of the posteromedial processes of the hyoid. The anterior region near the symphysis is, in the case

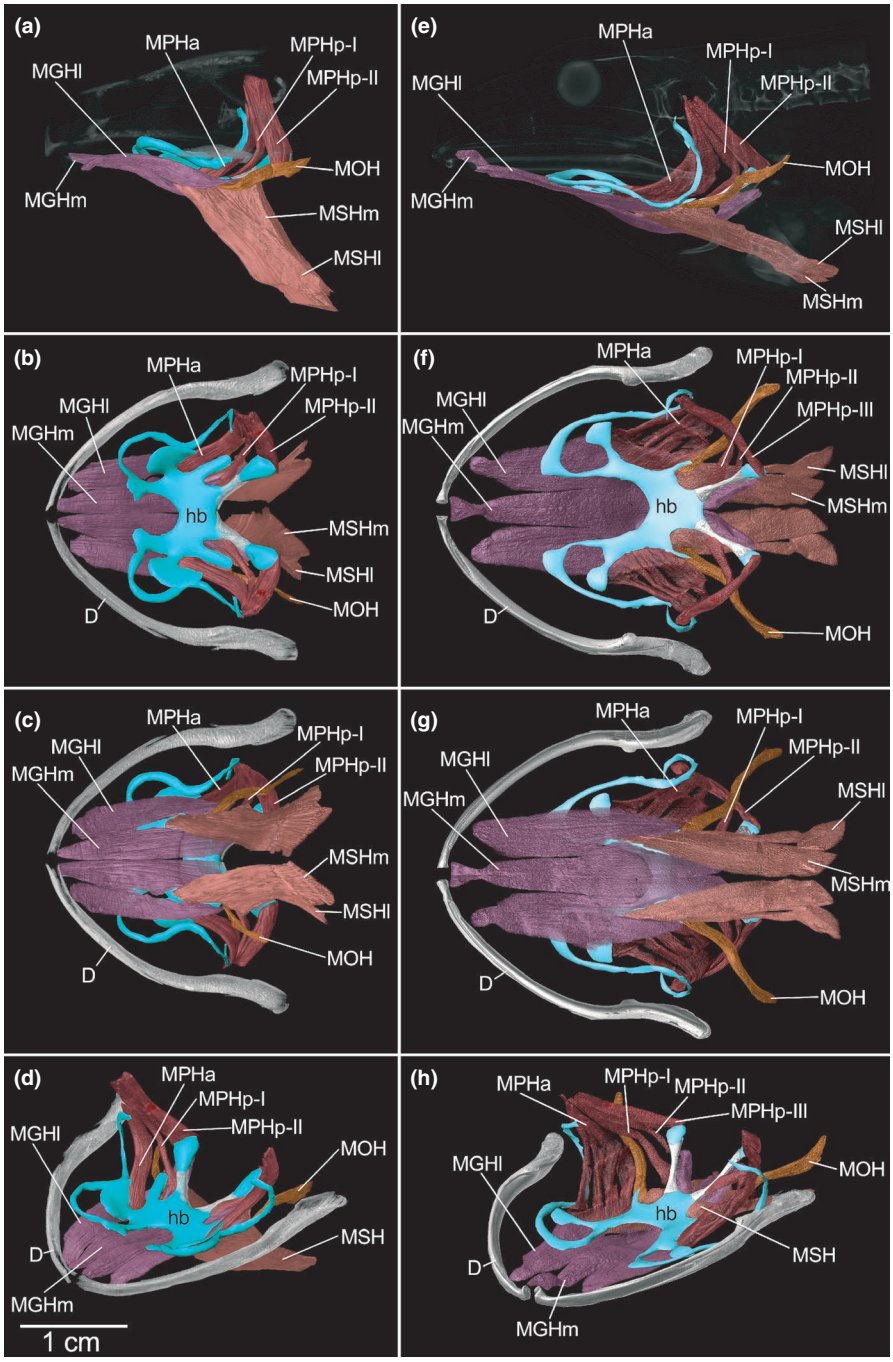

FIGURE 4 Hyoid apparatus and related musculature of *Calyptocephalella gayi* (a-d) and *Leptodactylus pentadactylus* (e-h) based on CT data. Osseous structures are visualized as volume rendering, cartilage and muscles based on segmentation-based rendering (surface or volume). (a and e) Lateral view; (b and f) dorsal view with lower jaw; (c and g) ventral view; (d and h) Oblique view from dorsolateral. D, dentale; hb, hyoid body; MGHl, musculus geniohyoideus lateralis; MGHm, musculus geniohyoideus medialis; MOH, musculus omohyoideus; MPHa, musculus petrohyoideus anterior; MPHp I-III, musculus petrohyoideus posterior I-III; MSHl, musculus sternohyoideus lateralis; MSHm, musculus sternohyoideus medialis. Scale bar applies for a-h

of *L.pentadactylus*, clearly separated by the m. genioglossus (MGG) pars ventralis (Figure 2f,g, Figure 4f,g), the posterior parts of the MGH are in both species separated from each other by the m. sternohyoideus (MSH), which fills the gap between these two muscles and inserts in the area of the anterolateral process (Figure 4c,g, Supplement 5). Median fibres of the MSH originate from the epicoracoid of the shoulder girdle, whereas the more lateral ones are a rostrad extension of the rectus abdominis muscles. Medial of the MGH lateralis, the MSH inserts near the lateral processes on the ventral side of the hyoid plate as well. The last muscle inserting on the ventral side of the hyoid body is the omohyoid muscle (MOH) (Figure 4a-h, Supplement 5). In *C.gayi*, this muscle originates from the distal inner side of the scapula, whereas in *L.pentadactylus* this muscle comes from the outer edge of the proximal area of the

scapula. In both frogs, this rather thin muscle inserts on the ventral side of the posterolateral process.

The ventrolateral side of the hyoid plate provides insertion areas for the petrohyoid muscles (MPH) (Figure 4a-h, Supplement 5). Both frogs have three portions of MPH, one anterior and two posterior ones, with the middle one being unilaterally split in two in *L.pentadactylus*. As mentioned before, the insertion area of the MPH anterior on the ventrolateral side of the hyoid between the lateral processes is notably larger in *L.pentadactylus* (Figure 4b,f). The same is true for the insertion area of the MPH posterior I on the posteromedial processes close to the hyoid plate. The MPH posterior II attaches directly to the distal ends of the posteromedial processes. The origin of the MPH posteriores is on the ventral side of the crista parotica. The anterior MPH originates directly at the fascia of MPH posterior I.

Most ventrally, three sets of muscles are present that also cover the ventral side of the hyoid muscles. These are the m. submentalis (MSM), m. intermandibularis (MIM) and the m. interhyoideus (MIH), which are similar in size and shape in both frogs (Figure 5). In *L.pentadactylus*, the MIM and the MIH are merged to form a continuous muscular layer. The MIM fibres run from the mandible medially to join in a large fascia in the ventral midline. The MIH fibres originate at the ends of the long hyale processes to insert at the midline fascia posterior of the MIM.

Concerning the tongue musculature (Figure 2), the MHG and the MGG are the two main muscles responsible for tongue motion and differ significantly in both species. In *C.gayi*, there are two portions of the MHG: a lateral portion, which originates from the ventral side close to the end of the posteromedial processes and proceeds into the lateral sides of the anterior half of the tongue. The medial bundle of the MHG comes from the proximal part of the posteromedial process and runs medially towards the most anterior part of the tongue (Figure 2c). In *L.pentadactylus*, two large portions arise from the distal ends of the posteromedial processes, join in the midline and remain united up to the hyoglossal sinus (Figure 2g). From there, several fibres run into different central regions of the tongue. In both frogs, muscle fascicles of the MHG and the MGG interdigitate with each other. However, in *C.gayi*, the bundles of the MHG are only located in the anterior part and do not reach the posterior part of the tongue (Figure 2a). In *L.pentadactylus*, the most dorsal bundles terminate in the posterior end of the tongue almost perpendicular to the tongue's surface and the MGG segments. The most ventral bundles end in the anterior region of the tongue and are oriented at an angle close to 45° to the tongue's surface in resting position (Figure 2e). The same is true for the tongue of *C.gayi*, but the MHG only inserts in the most anterior part of the tongue. The interdigitating parts of the MGG are more similar in the two frogs compared with the ones of the MHG. In *C.gayi*, there are slightly more and also thinner muscle fascicles, with some of them also reaching the lateral edges of the tongue, whereas in *L.pentadactylus* they all insert more centrally (Figure 2b,f). The main difference to *C.gayi* is that *L.pentadactylus* possesses a second part of the MGG, the MGG ventralis, which originates in the symphyseal region of the mandible. Thus, all the fibres of the MGG originate from the ventral part of the same muscle (Figure 2e-h).

4 | DISCUSSION

The recent MicroDECT technique (Supplement 1) allows a complete digital dissection and thus provides promising methods in comparative anatomy (see Supplements 7 and 8 for interactive 3D PDF's). Furthermore, such data can be used for additional computational biomechanical analyses. Based on detailed information on the musculoskeletal anatomy and muscle physiology, multibody dynamic analysis (MDA) can be used to simulate musculoskeletal function during feeding. Furthermore, it allows to calculate muscle forces, joint moments, joint reaction forces and bite forces based on in vivo observations of skull movements.

The results presented here demonstrate a detailed perspective on the musculoskeletal cranial system of two frog species. We used

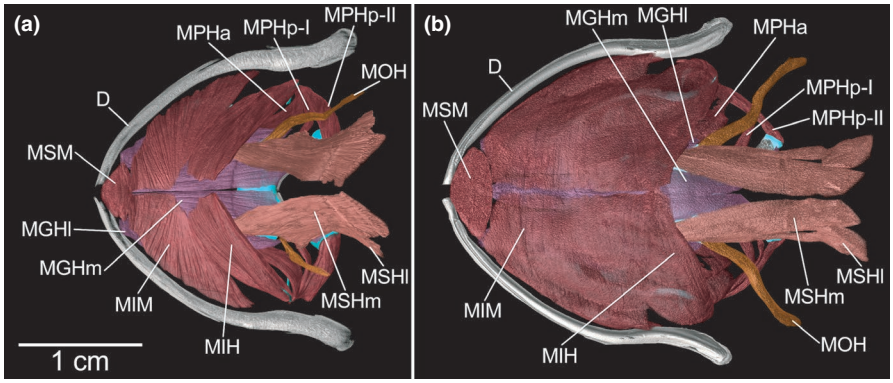

FIGURE 5 Ventral view of musculature of floor of mouth with underlying hyoid musculature of *Calyptocephalella gayi* (a) and *Leptodactylus pentadactylus* (b) based on CT data. Osseous structures are visualized as volume rendering, cartilage and muscles based on segmentation-based rendering (surface or volume). D, dentale; MGHl, musculus geniohyoideus lateralis; MGHm, musculus geniohyoideus medialis; MIH, musculus interhyoideus; MIM, musculus intermandibularis; MOH, musculus omohyoideus; MPHa, musculus petrohyoideus anterior; MPHp I-II, musculus petrohyoideus posterior I-II; MSHl, musculus sternohyoideus lateralis; MSHm, musculus sternohyoideus medialis; MSM, musculus submentalis. Scale bar applies for a-b

this description to gain insight into possible adjustments to the feeding medium and feeding mechanisms.

From an evolutionary perspective, facultative or obligate aquatic feeding in adult amphibians evolved secondarily since their last common ancestor most likely lived terrestrially (e.g. Deban et al., 2001; O'Reilly et al., 2002). Adult aquatic feeding frogs generally use modifications of terrestrial mechanisms, such as lunging at their prey and ingestion by jaw prehension. Only a few species of pipids and *Telmatobius* have re-evolved suction feeding (Barrionuevo, 2016; Carreño & Nishikawa, 2010; Cundall et al., 2017; O'Reilly et al., 2002). The only extant species of the genus *Calyptocephalella*, *C.gayi*, shows a fully aquatic lifestyle—although being able to feed in terrestrial environment—and also seems to use suction feeding (Wiesinger, 2017). In contrast, the genus *Leptodactylus* exemplifies the opposite evolution from a more riparian lifestyle to a terrestrial one, especially regarding their dependence on water for reproduction (De Sá et al., 2014; Heyer, 1969). Given the very distinct lifestyles of the two examined species, *C.gayi* exhibits several differences in its morphology that could be related to aquatic feeding when compared to the terrestrial *L.pentadactylus*. However, it should be noted that the two species used for comparison are not closely related and phylogenetically distant among neobratrachians. Hence, many of the observed differences can also be related to this distance, which ultimately would require to study more closely related representatives. Functional aspects related to the differences in the morphology of the two species are difficult to assess because several of the structures such as the hyoid, for example, have various functions, such as air circulation during breathing and vocalization, closing the nares or capturing and manipulating prey. These diverse functions may be in conflict with each other, and thus, morphology often represents a compromise and cannot only be assigned to a single function (Emerson, 1977; Regal & Gans, 1976; Trueb, 1993).

4.1 | The skull

The anuran skull is typically depressed with a large orbit in the temporal region, as in *C.gayi* and *L.pentadactylus*. It is even more simplified than that of salamanders and caecilians regarding the fusion and/or loss of dermal bones (for a more detailed description, see Nishikawa, 2000; Trueb & Alberch, 1985; Trueb, 1993; Schoch, 2014). The skull of *C.gayi* generally appears more robust due to the larger nasal, frontoparietal and squamosal. Thus, it resembles ancestral tetrapod forms with a completely closed skull roof, which allows different areas of origin for the adductor musculature. Most stem tetrapods show dermal bones that are conspicuously sculptured by tubercles, pits, ridges and furrows (Rinehart & Lucas, 2013; Trueb, 1993; Witzmann et al, 2010), similar to the skull of *C.gayi*, which is covered with tubercles, a sign of hyperossification. Hyperossification has evolved independently in several extant anurans but was absent at the ancestry of frogs (Paluh et al, 2020). The degree of skull ossification in anurans depends on their habitat (only 9% of aquatic species show hyperossification) and feeding style (feeders on vertebrate prey have hyperossified skulls and a strengthened skull yielding higher bite forces) and not on size (Paluh et al., 2020; Trueb, 1970).

Both examined frogs possess teeth-bearing vomers that show variation that is particularly common among neobatrachians. The vomers of *C.gayi* are less developed and are situated further rostral. Thus, the flat, streamlined palate is elongated, compared with the vaulted one of *L.pentadactylus*. Bramble and Wake (1985) have identified a flat palate as characteristic for aquatic feeding because it leaves more room for volume increase and facilitates smooth water flow during suction feeding.

4.2 | The hyoid apparatus

The overall structure of the hyoid in *C.gayi* and *L.pentadactylus* is similar to other described anurans. Compared with the hyobranchia of caecilians and salamanders, it is highly modified after metamorphosis (for overview, see Emerson, 1977; Fabrezi & Lobo, 2009; Gans & Gorniak, 1982; Nishikawa, 2000; Roth et al., 1990; Schwenk, 2000; Trueb, 1993). The most basic function of the hyoid is to support the tongue, but it also fulfils a crucial role in feeding and breathing as well as vocalization (Nishikawa, 2000; Roth et al., 1990). While the hyoid apparatus has a limited function in lingual prehension in anurans (Gans & Gorniak, 1982), it is indispensable for suction feeding (see Lauder, 1985; Lauder & Shaffer, 1993). Concerning hyoid and tongue dimensions, aquatic and terrestrial species show an inverse relationship in tetrapods with aquatic ones generally possessing large hyoids and less developed tongues, while the opposite is the case for terrestrial ones (Barrionuevo, 2016; Bramble & Wake, 1985; Lemell et al., 2000, 2002). This probably also applies to *C.gayi* and *L.pentadactylus*, as the former does indeed have a broader hyoid and a smaller tongue.

4.3 | The tongue

In its ancestral state, the anuran tongue contains voluntary muscles and can be slightly protruded out of the mouth (Deban & Nishikawa, 1992; Iwasaki, 2002; Nishikawa & Cannatella, 1991). *C.gayi* has a smaller tongue than *L.pentadactylus*. In the former, the tongue slightly exceeds half of the jaw size, while it reaches about 70% of the jaw length in the latter. Tongue reduction is not unusual in aquatic anurans and in extreme cases can even entail the entire lack of a tongue, as, for instance, in Pipidae (see Deban et al., 2001; Horton, 1982). Tongue reduction increases the expandable volume of the buccal cavity during suction feeding. Moreover, it causes a less turbulent flow of water and saves energy (Bramble & Wake, 1985). The physical constraint of water on the morphology of the feeding apparatus is strong, as the reduction of the tongue evolved convergently in aquatic anurans, salamanders and turtles (e.g. Bramble & Wake, 1985; Deban & Wake, 2000; Lemell et al., 2002). In terms of the overall size and associated muscles, terrestrial

anurans like *L.pentadactylus* tend to have larger tongues, since they need to overcome greater gravitational forces than in water and the larger contact area between tongue and prey also improves adhesive bonding (Bramble & Wake, 1985). Both *L.pentadactylus* and *C.gayi* are known for their ability to catch rather large prey (Hutchins et al., 2003). With respect to the above-mentioned tongue reductions in aquatic feeders and given that *C.gayi* barely uses its tongue in his natural aquatic environment, an even more reduced tongue could be expected in this species. Nevertheless, *C.gayi* is able to feed on land and use its tongue for terrestrial food uptake of larger prey (Wiesinger, 2017), which might explain the fact that its tongue is not further reduced.

4.4 | Related musculature

Despite the different densities of water versus air, the depressor mandibulae (MDM) of the aquatic *C.gayi* and the terrestrial *L.pentadactylus* show only a few differences. Lowering the mandible is also crucial for terrestrial species, as the opening of the mouth is necessary for tongue protraction, irrespective of the protraction mechanism (Mallet et al., 2001). Since both investigated species feed on land via mechanical pulling (Nishikawa, 1999), a similar shape of this muscle can be expected; nevertheless, we found different origins. The MDM of the aquatic *C.gayi* has a more fanlike shape with a broader area of origin at the scapula, resulting in longer posterior fibres. This pattern was also described in aquatic and semiaquatic species of *Telmatobius* (Barrionuevo, 2016). In contrast, the MDM of *L.pentadactylus* is rather compact and oriented in a more vertical direction.

The adductor muscle complex consisting of five individual muscles may be a way to circumvent the compromise between speed and strength of a muscle depending on the muscle's insertion. The insertions of the five individual adductor muscles are spread along the longitudinal axis on the posterior third of the mandible around the coronoid process, and each can take advantage of different lever properties (Kardong, 2012). The posterior adductors (MAM posterior and internus) allow for greater speed and the more anterior ones (MAM externus and longus) for greater bite force, enabling a more economic design. The MAM lateralis stretches in anteroposterior direction and is not assignable to either category, but functions as stabilizer of the jaw joint. There are obvious differences in the origins of the MAM longus and internus in *C.gayi* and *L.pentadactylus*. These differences are rooted in the distinct configuration of the skulls. *C.gayi*'s closed skull, more similar to amphibian temnospondyl ancestors, only permits two adductors to attach along the ventral side of the frontoparietal (Schoch, 2014). This hypothesis implies that the 'normal' fenestrated batrachian skull situation involved early bone fusion and true bone loss in order to permit a novel arrangement of jaw musculature. Tadpoles of *C.gayi*, like larval temnospondyls from early developmental stages onwards, bear large ornamented dermal bones like the frontoparietals (Muzzopappa & Nicoli, 2010; Reinbach, 1939), not permitting jaw musculature to attach on the dorsal side at any stage of development. In contrast, MAM longus and internus of *L.pentadactylus* expand onto the dorsal surface of the frontoparietal—representing the typical batrachian skull design—and even meet with the ones from the opposite side (MAM internus; Supplement 6).

The sternohyoid muscle (MSH) and its insertion to the hyoid (Supplement 5) are larger in *C.gayi* than in the terrestrial *L.pentadactylus* due to the greater forces needed by aquatic feeding anurans. In aquatic feeding, contraction of the MSH retracts the hyoid and therefore creates suction by expanding the buccal cavity. During lingual prehension, it indirectly supports the retraction of the tongue by retracting the hyoid (see Bramble & Wake, 1985; De Jongh & Gans, 1969; Emerson, 1977; Martin & Gans, 1972). Consequently, the activity of the MSH is different depending on the feeding medium. When feeding in water, the MSH should be active during the expansion phase, whereas in terrestrial feeding the high activity of the MSH starts in the retraction phase of the tongue (Gans & Gorniak, 1982). Considering the activity patterns of the MSH, *C.gayi* needs to be able to adjust the time points of activity depending on the medium in which it feeds. A similar variation in the build of the MSH has also been found in the comparative study on aquatic and semiaquatic species of *Telmatobius* (Barrionuevo, 2016).

Together with the petrohyoid (MPH) and the omohyoid (MOH) muscles, the geniohyoid musculature (MGH medialis and lateralis) is responsible for elevating the hyoid and thus involved in oral respiration, vocalization and feeding (De Jongh & Gans, 1969; Emerson, 1977; Kardong, 2012; Martin & Gans, 1972). This diversity of functions seems to balance their varying importance in aquatic and terrestrial species and may explain that only slight differences are present in *C.gayi* and *L.pentadactylus*. Only the MPH anterior is more prominent in *L.pentadactylus* and has a much larger insertion area along the lateral side of the hyoid plate between the antero- and posterolateral processes (Supplement 5). However, it is a rather thin sheet of muscle compared with the more compact one in *C.gayi*. The number of petrohyoid muscles in anurans varies between one and four pairs, including the MPH anterior (Duellman & Trueb, 1986; Gans & Gorniak, 1982; Ziermann & Diogo, 2014), with four pairs being the original state (Trewawas, 1933). Fully aquatic pipid species, as members of the base of the anuran tree, possess only one MPH, which may indicate that a reduction is related to suction feeding (Duellman & Trueb, 1986), but four pairs are present in the two suction feeding aquatic and semiaquatic *Telmatobius* species (Barrionuevo, 2016). Leptodactylids usually show three posterior MPH (Trewawas, 1933); our specimen was asymmetric with three on the right and just two on the left side, which could be an indication for a high inter- and intraspecific variability regarding this musculature.

The MIM and the MIH, which are responsible for raising the buccal floor (Fabrezi & Lobo, 2009; Gans & Gorniak, 1982; Nishikawa, 2000), are quite similar in *C.gayi* and *L.pentadactylus*. The most striking difference is that they form a continuous sheet in the latter, whereas they are clearly separable in the former. The relationship between these two muscles has usually been described in somewhat vague terms, and no explanations for the variations have been proposed, but both arrangements have been found (Gans & Gorniak, 1982; Johnston, 2011; Nishikawa, 2000).

Despite the variation in the anuran tongue morphology, there are several common features. Most importantly, the tongue is attached close to the mandibular symphysis in the front of the buccal cavity and has a protractor (MGG) and a retractor muscle (MHG), whose fibres run in parallel, but opposite directions along the length of the tongue (see Horton, 1982; Nishikawa, 2000; Regal & Gans, 1976). In general, as observed in the current study, the MHG displays less variation than the MGG, whose configuration ranges from unspecialised to quite complex (Horton, 1982). However, it seems that even simple forms of MGG allow frogs to protract their tongues for lingual prehension via mechanical pulling (Regal & Gans, 1976).

The diversity of the MGG structure can be organized in four distinct states according to Horton (1982); *C.gayi* exhibits the basic state I (found in hylids and in *Ascaphus*, *Pelobates*, *Pelodytes* and *Mixophyes*), and *L.pentadactylus* the more complex state II (found in *Dendrobates*, *Bufo*, *Capensibufo* and leptodactylid species). In state I, one genioglossal element, the interdigitating one, originates near the symphysis of the mandibles and runs caudally to interdigitate with the MHG, ultimately inserting into the tongue. In state II, an additional ventral part of the MGG is present, besides the interdigitating elements. It consists of rather short fibres forming a solid structure near the mandibular symphysis (Fabrezi & Lobo, 2009; Horton, 1982) and has been functionally described as a fulcrum that promotes tongue protraction (Gans & Gorniak, 1982; Nishikawa, 2000). The MGG ventralis is thus present in species with well-developed tongue protrusion mechanisms. Species like *Telmatobius* sp. or *C.gayi* with limited abilities of tongue protraction lack this additional element (Barrionuevo, 2016; Horton, 1982). Denervation studies of the MGG in terrestrial species lead to a marked decrease in the tongue's reach and height as well as the rate of successful capture attempts (for review, see Nishikawa, 2000). This indicates that the MGG is not only responsible for stiffening and supporting the tongue during protraction but also for fully protracting it. However, denervation of the MGG did not entirely prevent tongue protraction in some species, indicating that other muscles, like the MSM, are also partly involved in the movement rotating the tongue distally. It seems that mechanical pullers of the MGG basic state I, like *C.gayi*, use the MSM as additional force generating element for tongue protraction, whereas all other MGG states rely more on the ventral part of MGG as a fulcrum. The interdigitating part of the MGG is similar in the investigated species and in many other described ones (see Horton, 1982; Kleinteich & Gorb, 2015a; Nishikawa, 2000). The MGG splits into more segments in *C.gayi* than in *L.pentadactylus*, while the inverse situation is present in the MHG. The interdigitating pattern of the two muscles enables equally distributed forces, which is particularly important for the MHG. However, Johnston (2011), unlike Horton (1982), also detected intraspecific variation of this feature, thus limiting the value of interspecific comparison.

The MHG, located ventral of the hyoid, differs between *C.gayi* and *L.pentadactylus* mainly in size and origin on the hyoid's posteromedial process. The MHG is markedly larger, and its origin is more pronounced in the latter species. This may relate to their ability to use lingual prehension to catch rather large prey on land, which requires a strong retractor muscle (Kleinteich & Gorb, 2015a, 2015b; Nishikawa, 1999). Ideally, the fibres of the MHG act perpendicular to the surface of the prey in order to prevent peeling and the tongue being thereby detached from the prey. Consequently, distributing the fibres in an angle close to 90° to the tongue's surface enhances the tongue's adhesive strength and enables the transport of large prey into the mouth (Kleinteich & Gorb, 2015a, 2015b). This is realized in *L.pentadactylus* in contrast to *C.gayi* in which the MHG only stretches anteriorly but not over the whole surface of the tongue. It indicates that the species is less adapted to terrestrial feeding since the tongue is more likely to detach from the prey during retraction.

The resting position of the tongue in *C.gayi* and *L.pentadactylus* also differs according to the MHG. In the latter, the insertions of the fascicles are distributed over the whole tongue, while they do not reach the posterior end in the former. As a result, *C.gayi* lacks the ability to completely pull the free, posterior flap of the tongue ventrally in contrast to *L.pentadactylus*.

5 | CONCLUSIONS

Overall, the comparison of the anatomy of the feeding apparatus of the aquatic *C.gayi* and the terrestrial *L.pentadactylus* has shown several variations and distinct features that could be related to their respective habitat and way of feeding. As is typical for aquatic feeders, *C.gayi* has a comparatively small tongue, flat palate, well-developed hyoid and related muscles, especially the MSH. In contrast, the fibre distribution of the MHG and MGG in *L.pentadactylus* are better suited for lingual prehension. The intermandibular muscles, the MGH and MPH, are rather similar in both species. This might be related to their various functions apart from feeding, which are not restricted to either an aquatic or a terrestrial lifestyle. The adductor muscles mainly differ in size and the origins of MAM longus and internus, which are associated with the different skull structure in the two species. Interestingly, the fully aquatic *C.gayi* does not show typical reductions of specialized aquatic frogs like pipids, that is, further tongue reduction to aglossal combined with a reduction of tongue musculature, but this is due to the fact that *C.gayi* is still able to feed on land via lingual prehension. Although predominantly living and feeding in an aquatic habitat, *C.gayi* combines anatomical features of aquatic and terrestrial frogs.

Despite the diversity of feeding mechanisms, there are rather few morphological differences in the feeding apparatus of frogs that have, however, led to crucial biomechanical changes in feeding behaviour, especially with regard to tongue protraction (Nishikawa, 2000; Nishikawa & Gans, 1996). Such differences in the anatomy of frogs' feeding apparatus have been studied for decades (e.g. Haas, 2001; Horton, 1982; Trewavas, 1933), but the function of these variations during feeding still has not been clearly identified (Kleinteich & Gorb, 2015b; Nishikawa, 2000).

ETHICS APPROVAL AND CONSENT TO PARTICIPATE

The used specimen are loans of the collection of the Museum of Natural History, Vienna.

CONSENT FOR PUBLICATION

Not applicable.

ACKNOWLEDGEMENTS

We would like to thank the National History Museum Vienna for providing specimen of *C. gayi* and *L. pentadactylus* for the microCT scans. This research was supported using resources of the VetCORE Facility (Imaging) of the University of Veterinary Medicine Vienna. All authors have no conflict of interest to declare.

CONFLICT OF INTERESTS

The authors declare that they have no competing interests.

AUTHOR'S CONTRIBUTIONS

SK: data acquisition, reconstruction, analysis, text; VB: data acquisition, reconstruction, figures; TS: reconstruction, figures, text; SH: µCT scans, reconstruction, revision of text; CJB: conception, revision of text; PL: conception, design, text; All authors read and approved the final manuscript.

DATA AVAILABILITY STATEMENT

The data that support the findings of this study are available from the corresponding author upon reasonable request. Complete CT stacks can be found at MorphoSource:

http://www.morphosource.org/Detail/MediaDetail/Show/media_id/64614

http://www.morphosource.org/Detail/MediaDetail/Show/media_id/65016

http://www.morphosource.org/Detail/MediaDetail/Show/media_id/64613

http://www.morphosource.org/Detail/MediaDetail/Show/media_id/64285

ORCID

Patrick Lemell https://orcid.org/0000-0003-0262-4047

REFERENCES

Barrionuevo, J.S. (2016) Independent evolution of suction feeding in Neobatrachia: Feeding mechanisms of two species of *Telmatobius* (Anura: Telmatobiidae). *Anatomical Record*, 299, 181–196.

Bever, G.S., Bell, C.J. & Maisano, J.A. (2005) The ossified braincase and cephalic osteoderms of *Shinisaurus crocodilurus* (Squamata, Shinisauridae). *Palaeontol Electron*, 8.

Bramble, D.M. & Wake, D.B. (1985) Feeding mechanisms of lower tetrapods. In: Hildebrand, M., Bramble, D.M., Liem, K.F. and Wake, D.B. (Eds.) *Functional Vertebrate Morphology*. Cambridge, MA: The Belknap Press, pp. 230–261.

Brocklehurst, R., Porro, L., Herrel, A., Adriaens, D. & Rayfield, E. (2019) A digital dissection of two teleost fishes: comparative functional anatomy of the cranial musculoskeletal system in pike (*Esox lucius*) and eel (*Anguilla anguilla*). *Journal of Anatomy*, 235, 189–204.

Buttimer, S.M., Stepanova, N. & Womack, M.C. (2020) Evolution of the unique anuran pelvic and hind limb skeleton in relation to microhabitat, locomotor mode, and jump performance. *Integrative and Comparative Biology*, 60(5), 1330–1345.

Carpenter, K.E., Berra, T.M. & Humphries, J.M. (2004) Swim bladder and posterior lateral line nerve of the nurseryfish, *Kurtus gulliveri* (Perciformes: Kurtidae). *Journal of Morphology*, 260, 193–200.

Carreño, C.A. & Nishikawa, K.C. (2010) Aquatic feeding in pipid frogs: The use of suction for prey capture. *Journal of Experimental Biology*, 213, 2001–2008.

Cei, J.M. (1962) *Batracios de Chile*. Santiago de Chile: Ediciones de la Universidad de Chile.

Collings, A.J. & Richards, C.T. (2019) Digital dissection of the pelvis and hindlimb of the red-legged running frog, *Phlyctimantis maculatus*, using Diffusible Iodine Contrast Enhanced computed microtomography (DICE muCT). *PeerJ*, 7, e7003.

Cox, P.G. & Faulkes, C.G. (2014) Digital dissection of the masticatory muscles of the naked mole-rat, *Heterocephalus glaber* (Mammalia, Rodentia). *PeerJ*, 2, e448.

Cundall, D., Fernandez, E. & Irish, F. (2017) The suction mechanism of the pipid frog, Pipa pipa (Linnaeus, 1758). *Journal of Morphology*, 278, 1229–1240.

De Jongh, H.J. & Gans, C. (1969) On the mechanism of respiration in the bullfrog, *Rana catesbeiana*: a reassessment. *Journal of Morphology*, 127, 29–289.

De Sá, R.O., Grant, T., Camargo, A., Heyer, W.R., Ponssa, M.L. & Stanley, E. (2014) Systematics of the neotropical genus *Leptodactylus* Fitzinger, 1826 (Anura: Leptodactylidae): phylogeny, the relevance of non-molecular evidence, and species accounts. *South American Journal of Herpetology*, 9(Special Issue 1), 1–128.

Deban, S.M. & Nishikawa, K.C. (1992) The kinematics of prey capture and the mechanism of tongue protraction in the green tree frog *Hyla cinerea*. *Journal of Experimental Biology*, 170, 235–256.

Deban, S.M., O'Reilly, J.C. & Nishikawa, K.C. (2001) The evolution of the motor control of feeding in amphibians. *American Journal of Zoology*, 41, 1280–1298.

Deban, S.M. & Wake, D.B. (2000) Aquatic feeding in salamanders. In: Schwenk, K. (Ed.) *Feeding: Form, Function, and Evolution in Tetrapod Vertebrates*. San Diego: Academic Press, pp. 65–94.

Duellman, W.E. & Trueb, L. (1986) *Biology of Amphibians*. New York: McGraw-Hill.

Early, C.M., Morhardt, A.C., Cleland, T.P., Milensky, C.M., Kavich, G.M. & James, H.F. (2020) Chemical effects of diceCT staining protocols on fluid-preserved avian specimens. *PLoS One*, 15(9), e0238783.

Emerson, S.B. (1977) Movement of the hyoid in frogs during feeding. *The American Journal of Anatomy*, 149, 115–120.

Fabrezi, M. & Lobo, F. (2009) Hyoid skeleton, its related muscles, and morphological novelties in the frog *Lepidobatrachus* (Anura, Ceratophyridae). *Anatomical Record*, 292, 1700–1712.

Gans, C. & Gorniak, G.C. (1982) Functional morphology of lingual protrusion in marine toads (*Bufo marinus*). *The American Journal of Anatomy*, 163, 195–222.

Gignac, P.M., Kley, N.J., Clarke, J.A., Colbert, M.W., Morhardt, A.C., Cerio, D. et al. (2016) Diffusible iodine-based contrast-enhanced computed tomography (diceCT): an emerging tool for rapid, high-resolution, 3-D imaging of metazoan soft tissues. *Journal of Anatomy*, 228, 889–909.

Gray, L.A., O'Reilly, J.C. & Nishikawa, K.C. (1997) Evolution of forelimb movement patterns for prey manipulation in anurans. *Journal of Experimental Zoology*, 277, 417–424.

Haas, A. (2001) Mandibular arch musculature of anuran tadpoles, with comments on homologies of amphibian jaw muscles. *Journal of Morphology*, 247, 1–33.

Haas, A., Pohlmeyer, J., McLeod, D.S., Kleinteich, T., Hertwig, S.T., Das, I. et al. (2014) Extreme tadpoles II: the highly derived larval anatomy of *Occidozyga baluensis* (Boulenger, 1896), an obligate carnivorous tadpole. *Zoomorphology*, https://doi.org/10.1007/s00435-014-0226-7.

Handschuh, S., Beisser, C.J., Ruthensteiner, B. & Metscher, B.D. (2017) Microscopic dual energy CT (microDECT): a flexible tool for

multichannel ex vivo 3D imaging of biological specimens. *Journal of Microscopy*, 267, 3–26.

Handschuh, S., Natchev, N., Kummer, S., Beisser, C.J., Lemell, P., Herrel, A. et al. (2019) Cranial kinesis in the miniaturised lizard *Ablepharus kitaibelii* (Squamata: Scincidae). *Journal of Experimental Biology*, 222.

Heyer, W.R. (1969) The adaptive ecology of the species groups of the genus *Leptodactylus* (Amphibia, Leptodactylidae). *Evolution*, 23, 421–428.

Holliday, C.M., Tsai, H.P., Skiljan, R.J., George, I.D. & Pathan, S. (2013) A 3D interactive model and atlas of the jaw musculature of *Alligator mississippiensis*. *PLoS One*, 8, e62806.

Horton, P. (1982) Diversity and systematic significance of anuran tongue musculature. *Copeia*, 1982, 595–602.

Hutchins, M., Duellman, W.E. & Schlager, N. (2003). *Grzimek's Animal Life Encyclopedia, 2nd Edition, Volume 6 Amphibians*. Farmington Hills, MI: Gale.

Iwasaki, S. (2002) Evolution of the structure and function of the vertebrate tongue. *Journal of Anatomy*, 201, 1–13.

Jetz, W. & Pyron, A. (2018) The interplay of past diversification and evolutionary isolation with present imperilment across the amphibian tree of life. *Nature Ecology and Evolution*, 2, 850–858.

Johnston, P. (2011) Cranial muscles of the anurans *Leiopelma hochstetteri* and *Ascaphus truei* and the homologies of the mandibular adductors on lissamphibia and other gnathostomes. *Journal of Morphology*, 272, 1492–1512.

Jones, M.E.H., Button, D.J., Barrett, P.M. & Porro, L.B. (2019) Digital dissection of the head of the rock dove (*Columba livia*) using contrast-enhanced computed tomography. *Zoological Letters*, 5, 17.

Kardong, K.V. (2012) *Vertebrates: Comparative Anatomy, Function, Evolution*, 6th edition. New York: McCraw-Hill.

Keeffe, R. & Blackburn, D.C. (2020) Comparative morphology of the humerus in forward-burrowing frogs. *Biological Journal of the Linnean Society*, 131(2), 291–303.

Kleinteich, T. & Gorb, S.N. (2015a) Frog tongue acts as muscle-powered adhesive tape. *Royal Society Open Science*, 2, 150333.

Kleinteich, T. & Gorb, S.N. (2015b) The diversity of sticky frog tongues. Conference paper. Bruker micro CT Users meeting.

Klinkhamer, A.J., Wilhite, D.R., White, M.A. & Wroe, S. (2017) Digital dissection and three-dimensional interactive models of limb musculature in the Australian estuarine crocodile (*Crocodylus porosus*). *PLoS One*, 12, e0175079.

Lauder, G.V. (1985) Aquatic feeding in lower vertebrates. In: Hildebrand, M., Bramble, D.M., Liem, K.F. and Wake, D.B. (Eds.) *Functional Vertebrate Morphology*. Cambridge, MA: The Belknap Press, pp. 210–229.

Lauder, G.V. & Shaffer, H.B. (1993) Design of feeding systems in aquatic vertebrates: Major patterns and their evolutionary interpretations. In: Hanken, J. and Hall, B.K. (Eds.) *The Skull – Volume 3: Functional and Evolutionary Mechanisms*. Chicago: University of Chicago Press, pp. 113–149.

Lautenschlager, S., Bright, J.A. & Rayfield, E.J. (2014) Digital dissection - using contrast-enhanced computed tomography scanning to elucidate hard- and soft-tissue anatomy in the Common Buzzard *Buteo buteo*. *Journal of Anatomy*, 224, 412–431.

Lemell, P., Beisser, C.J. & Weisgram, J. (2000) Morphology and function of the feeding apparatus of *Pelusios castaneus* (Chelonia; Pleurodira). *Journal of Morphology*, 244, 127–135.

Lemell, P., Lemell, C., Snelderwaard, P., Gumbenberger, M., Wochesländer, R. & Weisgram, J. (2002) Feeding patters of *Chelus fimbriatus* (Pleurodira: Chelidae). *Journal of Experimental Biology*, 205, 1495–1506.

Maisano, J.A., Bell, C.J., Gauthier, J.A. & Rowe, T. (2002) The osteoderms and palpebral in *Lanthanotus borneensis* (Squamata: Anguimorpha). *Journal of Herpetology*, 36, 678–682.

Mallet, E.S., Yamaguchi, G.T., Birch, J.M. & Nishikawa, K.C. (2001) Feeding motor patterns in Anurans: insights from biomechanical modeling. *American Journal of Zoology*, 41, 1364–1374.

Martin, W.F. & Gans, C. (1972) Muscular control of the vocal tract during release signalling in the toad *Bufo valliceps*. *Journal of Morphology*, 137, 1–27.

Matthews, T. & du Plessis, A. (2016) Using X-ray computed tomography analysis tools to compare the skeletal element morphology of fossil and modern frog (Anura) species. *Palaeontologia Electronica*, 19.1.1T, 1–46.

Metscher, B.D. (2009) MicroCT for comparative morphology: simple staining methods allow high-contrast 3D imaging of diverse non-mineralized animal tissues. *BMC Physiology*, 9, 11.

Muzzopappa, P. & Nicoli, L. (2010) A glimpse at the ontogeny of the fossil neobatrachian frog *Calyptocephalella canqueli* from the Deseadan (Oligocene) of Patagonia, Argentina. *Acta Palaeontologica Polonica*, 55(4), 645–654.

Nishikawa, K.C. (1999) Neuromuscular control of prey capture in frogs. *Philosophical Transactions of the Royal Society of London. Series B: Biological Sciences*, 354, 941–954.

Nishikawa, K.C. (2000) Feeding in Frogs. In: Schwenk, K. (Ed.) *Feeding: Form, Function, and Evolution in Tetrapod Vertebrates*. San Diego: Academic Press, pp. 117–147.

Nishikawa, K.C. & Cannatella, D.C. (1991) Kinematics of prey capture in the tailed frog *Ascaphus truei* (Anura: Ascaphidae). *Zoological Journal of the Linnean Society*, 103, 289–307.

Nishikawa, K.C. & Gans, C. (1996) Mechanisms of tongue protraction and narial closure in the marine toad *Bufo marinus*. *Journal of Experimental Biology*, 199, 2511–2529.

O'Reilly, J.C., Deban, S.M. & Nishikawa, K.C. (2002) Derived life history characteristics constrain the evolution of aquatic feeding behaviour in adult amphibians. In: Aerts, P., D'Août, K., Herrel, A. and Van Damme, R. (Eds.) *Topics in Functional and Ecological Vertebrate Morphology*. Maastricht: Shaker Publishing, pp. 153–190.

Paluh, D.J., Stanley, E.L. & Blackburn, D.C. (2020) Evolution of hyperossification expands skull diversity in frogs. *Proceedings of the National Academy of Sciences*, 117(15), 8554–8562.

Polcyn, M.J., Rogers, J.V.J., Kobayashi, Y. & Jacobs, L.L. (2002) Computed tomography of an Anolis lizard in Dominican amber: systematic, taphonomic, biogeographic, and evolutionary implications. *Palaeontol Electron*, 5, 1–13.

Porro, L.B. & Richards, C.T. (2017) Digital dissection of the model organism *Xenopus laevis* using contrast-enhanced computed tomography. *Journal of Anatomy*, 231, 169–191.

Pyron, R.A. & Wiens, J.J. (2011) A large-scale phylogeny of amphibia including over 2800 species, and a revised classification of extant frogs, salamanders, and caecilians. *Molecular Phylogenetics and Evolution*, 61, 543–583.

Regal, P.J. & Gans, C. (1976) Functional aspects of the evolution of frog tongues. *Evolution*, 30, 718–734.

Reinbach, W. (1939). Untersuchungen über die Entwicklung des Kopfskeletts von Calyptocephalus gayi. *Jenaische Zeitschrift für Naturwissenschaft*, 72, 211–362.

Rinehart, L.F. & Lucas, S.G. (2013). The functional morphology of dermal bone ornamentation in temnospondyl amphibians. In: Tanner, L.H., Spielmann, J.A. & Lucas, S.G. editors. *The triassic system*. vol. 61. Albuquerque: New Mexico Museum of Natural History; pp 524-532.

Roth, G., Nishikawa, K.C., Wake, D.B., Dicke, U. & Matsushima, T. (1990) Mechanics and neuromorphology of feeding in amphibians. *Netherlands Journal of Zoology*, 40, 115–135.

Rowe, T.B., Eiting, T.P., Macrini, T.E. & Ketcham, R.A. (2005) Organization of the olfactory and respiratory skeleton in the nose of the gray short-tailed opossum *Monodelphis domestica*. *Journal of Mammalian Evolution*, 12, 303–336.

Schoch, R.R. (2014) Amphibian skull evolution: The developmental and functional context of simplification, bone loss and heterotopy. *Journal of Experimental Zoology. Part B, Molecular and Developmental Evolution.*, 9999B, 1–12.

Schwarz, D., Konow, N., Roba, Y.T. & Heiss, E. (2020) A salamander that chews using complex, three-dimensional mandible movements. *Journal of Experimental Biology*, 223.

Schwenk, K. (2000) An introduction to tetrapod feeding. In: Schwenk, K. (Ed.) *Feeding: Form, Function, and Evolution in Tetrapod Vertebrates*. San Diego: Academic Press, pp. 21–61.

Sullivan, S.P., McGechie, F.R., Middleton, K.M. & Holliday, C.M. (2019) 3D muscle architecture of the pectoral muscles of European Starling (*Sturnus vulgaris*). *Integrative Organismal Biology*, 1, 1–18.

Trewavas, E. (1933) The hyoid and larynx of the Anura. *Philosophical Transactions of the Royal Society of London. Series B, Biological Sciences*, 222, 401–527.

Trueb, L. (1970) Evolutionary relationships of casque-headed tree frogs with co-ossified skulls (family Hylidae). *University of Kansas publications, Museum of Natural History*, 18(7), 547–716.

Trueb, L. (1993) Patterns of cranial diversity among the lissamphibia. In: Hanken, J. and Hall, B.K. (Eds.) *The Skull – Volume 2: Patterns of Structural and Systematic Diversity*. Chicago: University of Chicago Press, pp. 255–343.

Trueb, L. & Alberch, P. (1985). Miniaturization and the anuran skull: a case study of heterochrony. In: Duncker, H.R. & Fleischer, G. editors. *Functional Morphology in Vertebrates: proceedings of the 1st International Symposium on Vertebrate Morphology, Giessen, 1983*. Stuttgart: Gustav Fischer Verlag. pp 113-121.

Tykoski, R.S., Rowe, T.B., Ketcham, R.A. & Colbert, M.W. (2002) *Calsoyasuchus valliceps*, a new crocodyliform from the Early Jurassic Kayenta Formation of Arizona. *Journal of Vertebrate Paleontology*, 22, 593–611.

Wampula, T. (2015) La rana grande chilena: der Chilenische Helmkopf, *Calyptocephalella gayi*. *Aquaristik Fachmagazin: Aqua, Terra, Teich*, 47, 80–85.

Wiesinger, V. (2017) Feeding mechanism of *Calyptocephalella gayi*. Diploma thesis. University of Vienna.

Witzmann, F., Scholz, H., Müller, J. & Kardjilov, N. (2010) Sculpture and vascularization of dermal bones, and the implications for the physiology of basal tetrapods. *Zoological Journal of the Linnean Society*, 160, 302–340.

Zhang, M., Chen, X., Ye, C., Fei, L., Li, P., Jiang, J. et al. (2019) Osteology of the Asian narrow-mouth toad *Kaloula borealis* (Amphibia, Anura, Microhylidae) with comments on its osteological adaptation to fossorial life. *Acta Zoologica*, 2019(00), 1–18.

Ziermann, J.M. & Diogo, R. (2014) Cranial muscle development in frogs with different developmental modes: direct development versus biphasic development. *Journal of Morphology*, 275, 398–413.

SUPPORTING INFORMATION

Additional supporting information may be found online in the Supporting Information section.

How to cite this article: Kunisch S, Blüml V, Schwaha T, Beisser CJ, Handschuh S, Lemell P. Digital dissection of the head of the frogs *Calyptocephalella gayi* and *Leptodactylus pentadactylus* with emphasis on the feeding apparatus. *J Anat*. 2021;239:391–404. https://doi.org/10.1111/joa.13426